Phenomenology of Matching Exponentiated Photonic Radiation to a QED-Corrected Parton Shower in KKMChh

Scott Yost

The Citadel

The Military College of South Carolina

KKMChh was created in collaboration with S. Jadach (deceased), B.F.L. Ward and Z. Wąs.

Computational resources were provided by the Institute of Nuclear Physics, IFJ-PAN, Krakow. Assistance has been provided by A. Siodmok.

KKMChh

KKMChh is a precision Monte Carlo program for photonic and electroweak radiative corrections to hadron scattering, implementing the amplitude level exponentiation originally developed for electron-positron scattering at the quark level, modeling initial and final state QED radiation as well as initial-final interference to all orders in a soft-photon approximation, adding hard photon corrections through second order next-to-leading logarithm.

KKMChh includes initial state radiation (ISR), final state radiation (FSR), and initial-final interference (IFI) in addition to electro-weak radiative corrections tabulated using the DIZET-2.45 library.

For details, see S. Jadach, B.F.L. Ward, Z, Wąs and S.A. Yost,

- Phys. Rev. D94 (2016) 074006 [arXiv:1608.01260]
- Phys. Rev. D99 (2019) 076016 [arXiv:1707.06502]

NISR

The ab-initio photonic ISR in KKMChh is applied to an event with quarks generated using parton distribution functions which may already include QED effects. This can come from QED "contamination" in the input data for PDF sets including only QCD evolution, or from explicit photon generation in QED-corrected PDF sets.

NISR (negative ISR) is a mechanism added to KKMChh to back out ISR that would double-count QED radiation already accounted for in the PDF set.

The mechanism was described in a previous ICHEP talk. See S. Yost, et. al, *KKMChh: matching CEEX photonic ISR to a QED-corrected parton shower*, PoS(ICHEP2022)887 [arXiv:2211.17177].

We will briefly summarize NISR and then show its on a measurement of phenomenological interest, the forward-backward asymmetry $A_{\mathbf{FB}}$ in proton-proton collisions at the LHC.

QED-Corrected Joint Parton Luminosity Distributions

The starting point for understanding NISR is the parton joint luminosity distribution,

$$xL_{q\bar{q}}(\hat{x}s) \equiv \int dx_q dx_{\bar{q}}\, \delta(\hat{x} - x_q x_{\bar{q}}) f_q(x_q, \hat{x}s) f_{\bar{q}}(x_{\bar{q}}, \hat{x}s)$$

in terms of parton distribution functions $f_q(x_q, p^2), f_{\bar{q}}(x_{\bar{q}}, p^2)$ with quark momentum fractions $x_q, x_{\bar{q}}$ at CM energy $\sqrt{\hat{x}s}$. With exponentiated QED ISR, this becomes

$$xL_{q\bar{q}}^{\rm QED}(xs) = \int_0^{1-x} dv \int_x^1 d\hat{x}\, \delta\left(\hat{x} - \frac{x}{1-v}\right) \left[\hat{x}L_{q\bar{q}}(\hat{x}s)\right] \left[(1-v)\rho_{\rm ISR}^{(0)}(v, \hat{x}s)\right]$$

in terms of the luminosity function $L_{q\bar{q}}(\hat{x}s)$ at $\hat{x} = x/(1-v)$ and YFS-exponentiated ISR radiator

$$\rho_{ISR}^{(0)}(v,\, \hat{x}s) = F_{\rm YFS}(\gamma)\gamma v^{\gamma-1}, \quad F_{\rm YFS}(\gamma) = \frac{e^{-C_E\gamma}}{\Gamma(1+\gamma)},$$

$$\gamma = \gamma_{\rm ISR}(\hat{x}s, Q_q, m_q) = \frac{2\alpha}{\pi} Q_q^2 \left[\ln\left(\frac{\hat{x}s}{m_q^2}\right) - 1\right]$$

where $C_E = 0.5772\ldots$ is the Euler-Mascheroni constant and we use current quark masses $m_d = 4.7$ MeV, $m_u = 2.2$ MeV, $m_s = 150$ MeV, $m_c = 1.2$ GeV, $m_b = 4.6$ GeV.

These graphs show the ratio of NNPDF $xL(x)$ with QED corrections to without in a region around the Z pole used in many applications, and on a wider scale from 5 GeV to 1 TeV.

At $M_{q\bar{q}} = M_Z$, QED ISR reduces xL by -1.2% for the up quark and -0.29% for the down quark. The correction factor varies slowly over this range, mostly affecting normalization. (The inclusive Drell-Yan invariant mass distribution is reduced by a nearly flat $\sim 0.5\%$ in this range.)

The up quark correction varies from $+0.61\%$ to -4.2% over the wider range, while the down quark correction varies much less, from $+0.15\%$ to -1.0%.

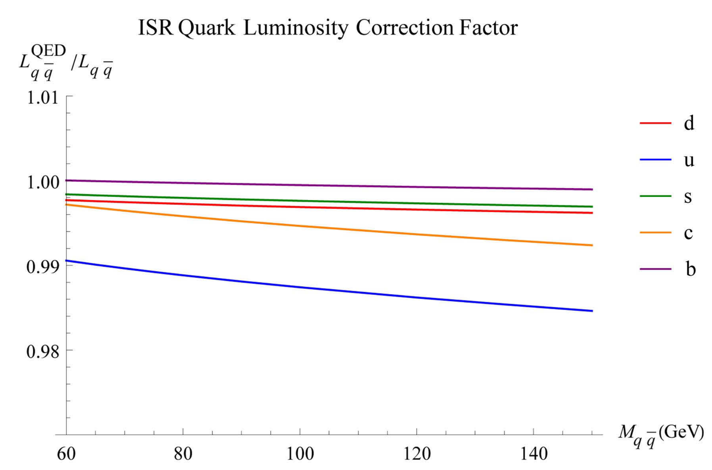

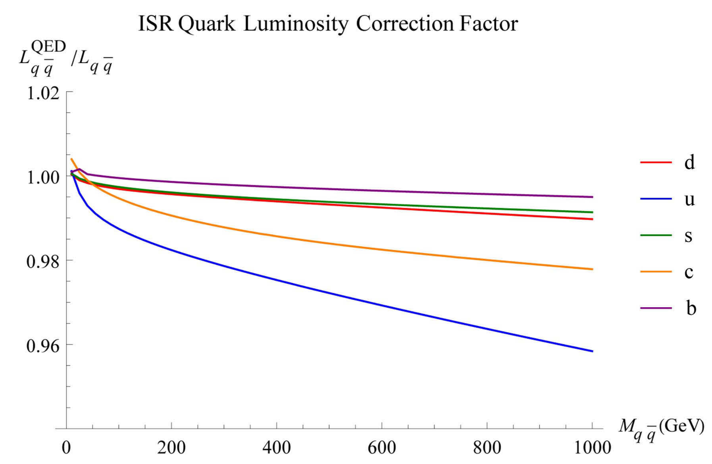

Matching KKMChh to QED-Corrected PDFs

The goal of NISR is to have a PDF that represents the full data, modeled with QCD and QED together, below the scale Q_0 but subtracts the QED component from $Q > Q_0$, where KKMChh will model the QED evolution.

For a process at a hard scale sx, we take $Q_0^2 = sx$ so that KKMChh starts with a pruned PDF at a higher scale before radiating its ISR. For a standard PDF set, Q_0 may be taken to be the starting point of QCD evolution.

Either way, the leading dependence on quark masses is canceled.

The net effect is to make a convolution of each quark PDF with a "half-radiator" $\rho_{\rm ISR}\left(-\frac{1}{2}\gamma_{\rm ISR}(xs), u_1\right)$ and $\rho_{\rm ISR}\left(-\frac{1}{2}\gamma_{\rm ISR}(xs), u_2\right)$, the convolution of which makes a full reverse radiator function. This introduces two more variables u_1, u_2 in the primary distribution, with the constraints $x = \hat{x}(1-u_1)(1-u_2)$.

The modified ISR energy fraction used in the MC generation becomes v' satisfying

$$(1-v') = (1-v)(1-u_1)(1-u_2)$$

and the quark energy fractions become

$$x_1(1-u_1), \qquad x_2(1-u_2).$$

With NISR, there are 6 variables in the KKMChh primary MC distribution to generate the quark flavor and the variables $\hat{x}, x_1, v, u_1$, and u_2.

See PoS (ICHEP2022) 887 [arXiv:2211.17177] for further details.

Forward-Backward Asymmetry Calculations

The remainder of this poster focuses on the calculation of the forward-backward asymmetry $A_{\mathbf{FB}}$ in proton-proton collisions, defined in the "Collins-Soper" frame.

We use two different PDF sets, NNPDF-3.1 with only QCD evolution starting from a scale of 2GeV and NNPDF-3.1-LuxQED, which includes both QCD and QED evolution.

For NNPDF-3.1, we calculate $A_{\mathbf{FB}}$ both with and without NISR applied at the starting scale 2GeV. For NNPDF-3.1-LuxQED, we calculate $A_{\mathbf{FB}}$ with NISR at the CM scale of the generated event.

KKMChh generated muon final states in proton collisions at an 8 TeV CM energy. No hadronic shower was applied to these events and no "cuts" were applied to the fermions.

All events include final state radiation (FSR). Initial state radiation (ISR) can be included or not, as can initial-final interference (IFI), allowing the size of these effects to be examined independently.

A sample of 10.4 billion events was generated without NISR, while 9.4 billion events were generated with NNPDF-3.1 and NISR at 2GeV, and 8.3 billion events were generated with NNPDF-3.1-LuxQED and NISR at the hard process scale.

The Effect of NISR on the $A_{\rm FB}$ Calculation

Invariant Mass Distributions

The first plot to the right shows the dependence of $A_{\mathbf{FB}}$ on the final lepton (muon) invariant mass M_{ll} for the three cases in the tables: NNPDF-3.1 without NISR (green), NNPDF-3.1 with NISR at 2GeV (blue) and NNPDF-3.1-LuxQED with NISR at the generated CM energy.

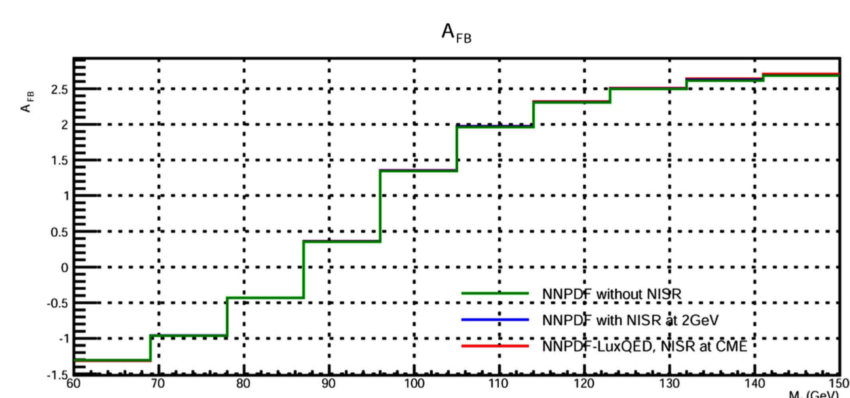

The second plot to the right shows the differences between each version with NISR and the version without NISR, as in the tables.

The shifts from adding NISR are mostly comparable for both versions.

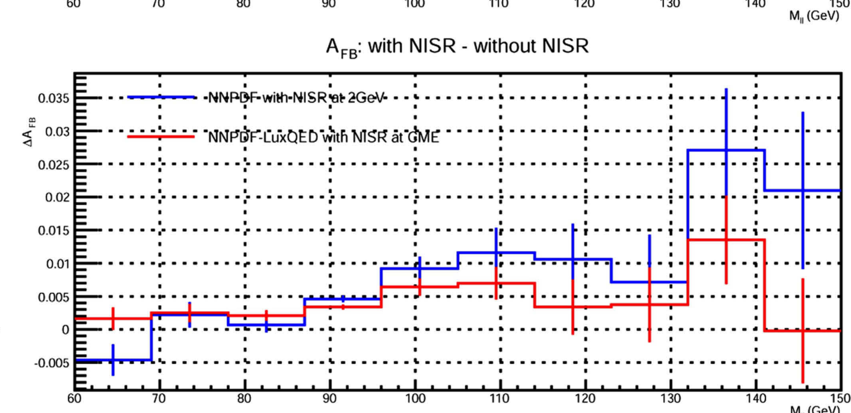

Rapidity Distributions

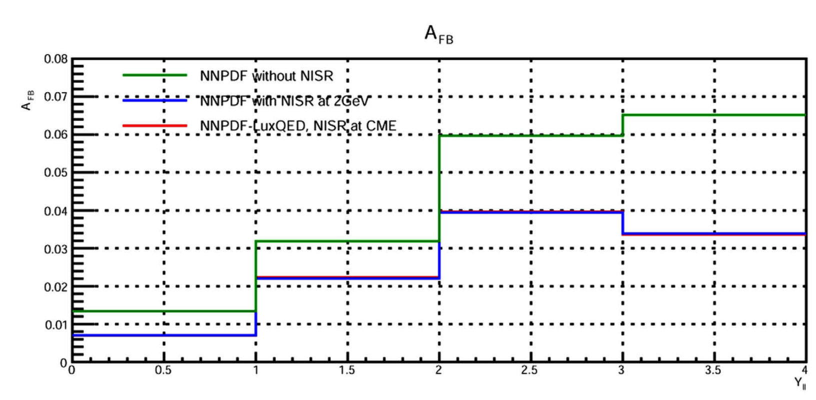

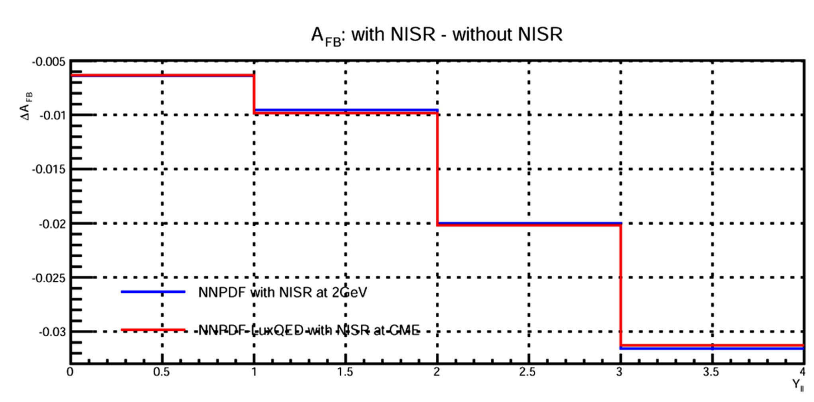

The first plot to the left shows the dependence of $A_{\mathbf{FB}}$ on the final lepton (muon) rapidity Y_{ll} for the three cases in the tables: NNPDF-3.1 without NISR (green), NNPDF-3.1 with NISR at 2GeV (blue) and NNPDF-3.1-LuxQED with NISR at the generated CM energy.

The second plot to the left shows the differences between each version with NISR and the version without NISR, as in the tables.

The shifts from adding NISR increase for larger rapidity and are generally comparable for the two versions.

(These plots include error bars but they are very small.)

Effect of NISR on Forward-Backward Asymmetry

This table shows three ways of calculating the forward-backward asymmetry $A_{\mathbf{FB}}$: version (1) using the standard NNPDF-3.1 PDF set without applying NISR, version (2) using the standard NNPDF-3.1 PDF set with NISR applied at 2GeV, the starting point for QCD evolution, and version (3) using NNPDF-3.1-LUXQED with NISR applied at the CM energy generated for the process.

$A_{\rm FB}$ in M_{ll} bins	89-93 GeV	60-120 GeV	60-81 GeV	81-101 GeV	101-150 GeV
(1) NNPDF, no NISR	0.03092(1)	0.02071(1)	-0.10869(4)	0.02886(1)	0.2186(1)
(2) NNPDF, NISR @ 2GeV	0.03128(4)	0.02109(4)	-0.10853(9)	0.02925(3)	0.2192(1)
(3) NNPDF-LuxQED, NISR	0.03135(6)	0.02115(4)	-0.1088(1)	0.02934(5)	0.2198(2)
NISR Difference (2) – (1)	0.00036(4)	0.00038(4)	0.0002(1)	0.00038(3)	0.0007(2)
NISR Difference (3) – (1)	0.00043(6)	0.00044(5)	-0.0001(1)	0.00047(5)	0.0012(2)

The results are binned in the final fermion (muon) invariant mass M_{ll}, first in a narrow bin around M_Z, then a wide bin, then three ranges between 60 and 150 GeV.

The effect of NISR on $A_{\mathbf{FB}}$ is most significant near M_Z. The two methods of applying NISR yield compatible results within the errors of the MC calculations.

NISR Effect on the ISR Contribution to $A_{\rm FB}$

This plot shows the dependence of the ISR contribution to $A_{\mathbf{FB}}$ on the final lepton (muon) invariant mass M_{ll} for the three cases in the tables: NNPDF-3.1 without NISR (green), NNPDF-3.1 with NISR at 2GeV (blue) and NNPDF-3.1-LuxQED with NISR at the generated CM energy.

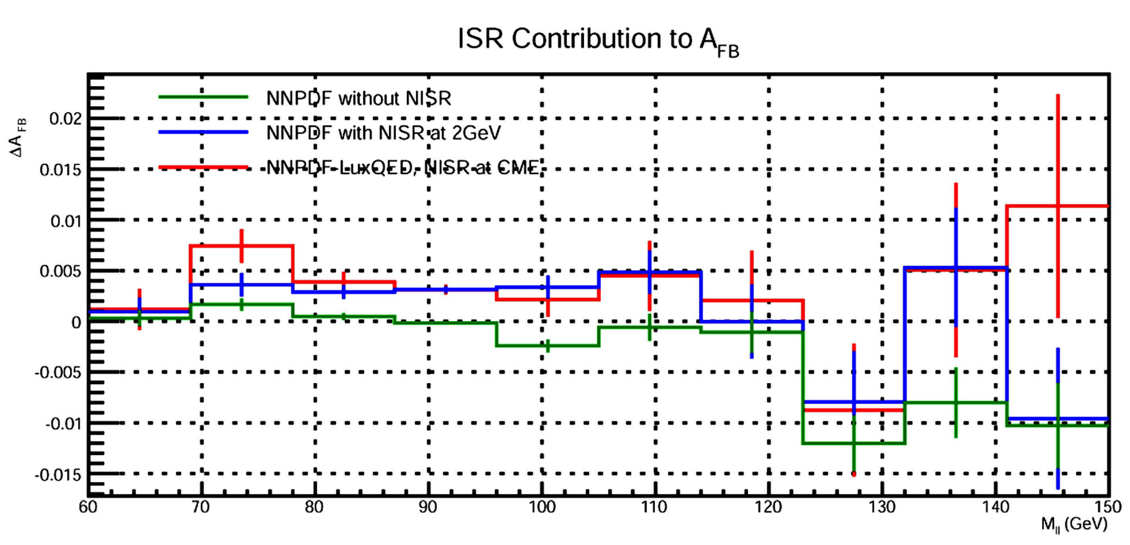

The shift from NISR is usually significant and the two versions with NISR are mostly compatible within the errors of the calculation.

NISR Effect on the ISR Contribution to $A_{\rm FB}$

This plot shows the dependence of the ISR contribution to $A_{\mathbf{FB}}$ on the final lepton (muon) rapidity Y_{ll} for the three cases in the tables: NNPDF-3.1 without NISR (green), NNPDF-3.1 with NISR at 2GeV (blue) and NNPDF-3.1-LuxQED with NISR at the generated CM energy.

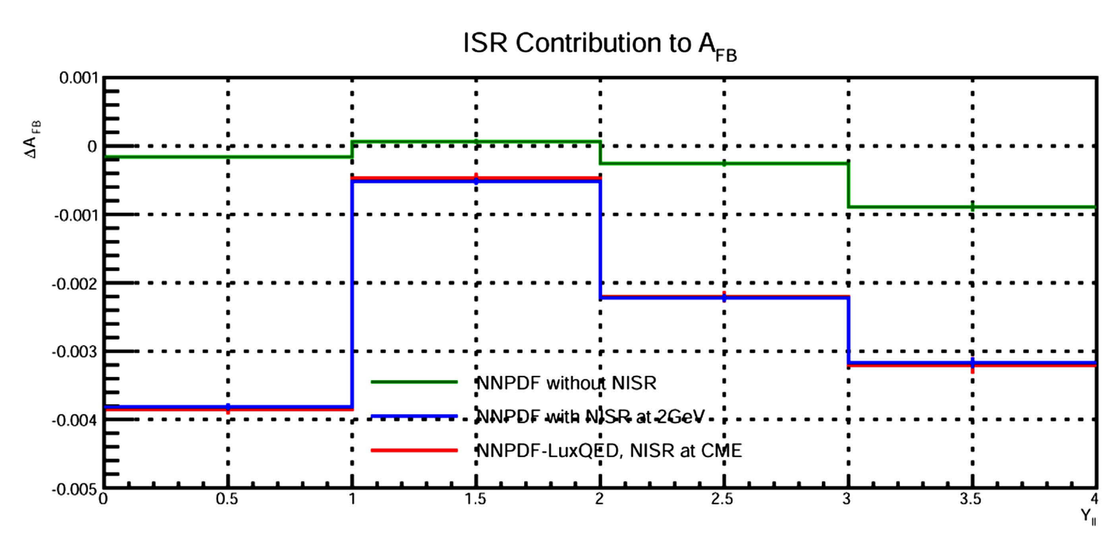

The shift from NISR is always significant and the two versions with NISR are compatible within the errors of the calculation. (This plot includes error bars but are very small.)

Effect of NISR on ISR and IFI Contribution to $A_{\rm FB}$

These tables show the contribution of ISR and IFI separately to the forward-backward asymmetry. IFI is turned off to calculate the ISR contribution from the difference between a calculation including ISR and FSR and one including FSR only. The IFI contribution is defined to be the difference between a calculation with IFI on and one with IFI off but including both ISR and FSR.

ISR Contribution to $A_{\rm FB}$ x 10^4	89-93 GeV	60-120 GeV	60-81 GeV	81-101 GeV	101-150 GeV
(1) NNPDF, no NISR	0.7(1)	0.1(1)	1.0(5)	0.1(1)	-4.0(8)
(2) NNPDF, NISR @ 2GeV	0.8(1)	3.7(3)	2.3(8)	3.8(3)	2(1)
(3) NNPDF-LuxQED, NISR	1.0(2)	3.7(4)	5(1)	3.6(4)	1(2)
Difference (2) - (1)	3.5(4)	3.6(3)	1.3(9)	3.7(3)	6(2)
Difference (3) - (1)	2.6(6)	3.6(4)	4(1)	3.5(5)	5(2)

IFI Contribution to $A_{\rm FB}$ x 10^4	89-93 GeV	60-120 GeV	60-81 GeV	81-101 GeV	101-150 GeV
(1) NNPDF, no NISR	0.7(1)	0.48(2)	1.4(1)	1.16(2)	-23.2(1)
(2) NNPDF, NISR @ 2GeV	0.8(1)	6.3(8)	1.6(3)	1.27(8)	-22.2(4)
(3) NNPDF-LuxQED, NISR	1.0(2)	0.5(1)	1.2(3)	1.3(1)	-24.5(6)
Difference (2) - (1)	0.1(2)	0.15(8)	0.2(3)	0.11(8)	1.0(4)
Difference (3) - (1)	0.3(2)	0.1(1)	-0.2(3)	0.1(1)	-1.3(6)

In most cases, the two versions with NISR yield compatible differences with respect to no NISR.

NISR Effect on the IFI Contribution to $A_{\rm FB}$

This plot shows the dependence of the IFI contribution to $A_{\mathbf{FB}}$ on the final lepton (muon) invariant mass M_{ll} for the three cases in the tables: NNPDF-3.1 without NISR (green), NNPDF-3.1 with NISR at 2GeV (blue) and NNPDF-3.1-LuxQED with NISR at the generated CM energy.

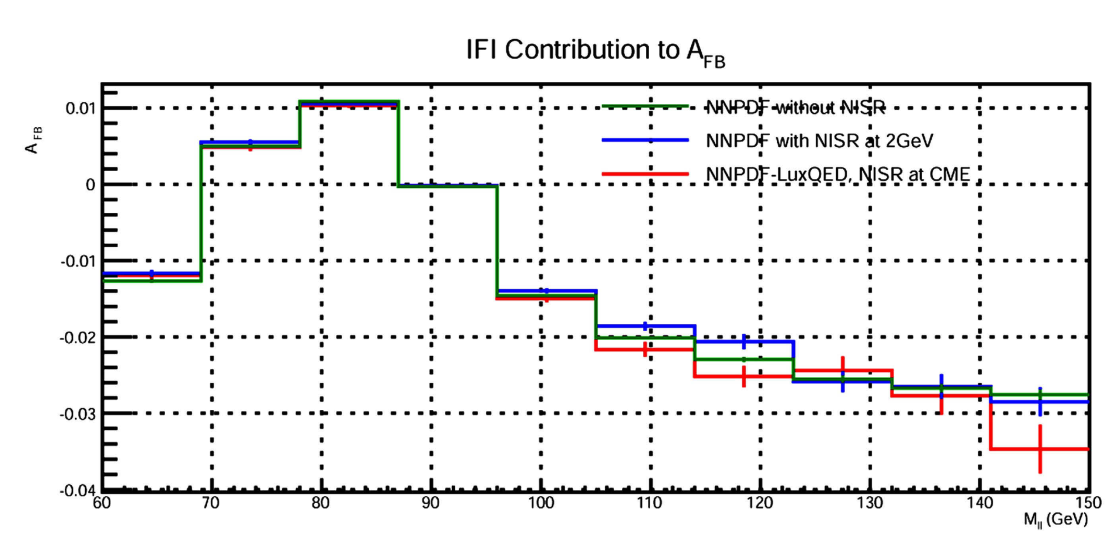

The shift from NISR becomes more significant away from M_Z. The two versions with NISR are not always in agreement for high invariant mass.

NISR Effect on the IFI Contribution to $A_{\rm FB}$

This plot shows the dependence of the IFI contribution to $A_{\mathbf{FB}}$ on the final lepton (muon) rapidity Y_{ll} for the three cases in the tables: NNPDF-3.1 without NISR (green), NNPDF-3.1 with NISR at 2GeV (blue) and NNPDF-3.1-LuxQED with NISR at the generated CM energy.

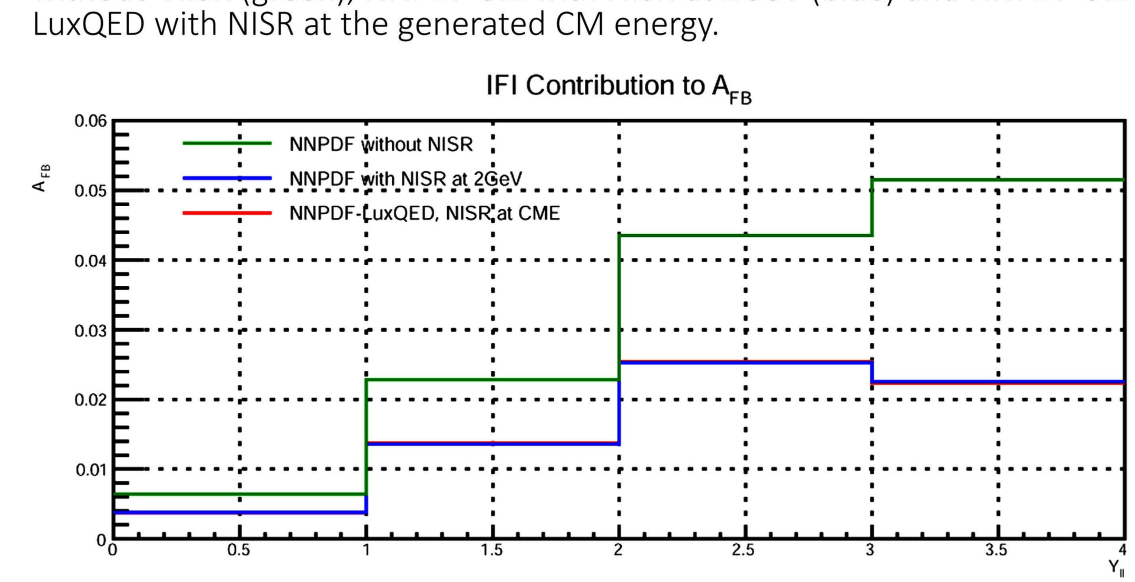

The shift from NISR is becomes more significant at high rapidity, and both versions with NISR are always comparable. (This plot includes error bars but they are very small.)